Analytical Methods

Selective determination of sulphide based on fluorescence quenching of MPA-capped CdTe nanocrystals by exploiting a gas-diffusion multipumping flow method

Journal:	*Analytical Methods*
Manuscript ID:	AY-ART-08-2014-001823
Article Type:	Paper
Date Submitted by the Author:	01-Aug-2014

Complete List of Authors:	Rodrigues, S.Sofia; Requimte, University of Porto, Faculty of Pharmacy, Department of Chemistry, Laboratory of Applied Chemistry Oleksiak, Zuzanna; The University of Warsaw, Department of Chemistry Ribeiro, David; Requimte, University of Porto, Faculty of Pharmacy, Department of Chemical Sciences, Laboratory of Applied Chemistry Poboży, Ewa; The University of Warsaw, Department of Chemistry Trojanowicz, Marek; The University of Warsaw, Department of Chemistry Prior, João; Requimte, Faculty of Pharmacy of University of Porto, Department of Chemical Sciences, Laboratory of Applied Chemistry Santos, Joao; Requimte, University of Porto, Faculty of Pharmacy, Department of Chemistry, Laboratory of Applied Chemistry; Requimte, Faculty of Pharmacy of University of Porto, Department of Chemical Sciences, Laboratory of Applied Chemistry

Selective determination of sulphide based on photoluminescence quenching of MPA-capped CdTe nanocrystals by exploiting a gas-diffusion multi-pumping flow method

S. Sofia M. Rodrigues[a], Zuzanna Oleksiak[b], David S. M. Ribeiro*[a], Ewa Poboży[b], Marek Trojanowicz[b], João A.V. Prior[a], João L. M. Santos*[a]

[a] *Requimte, Department of Chemical Sciences, Laboratory of Applied Chemistry, Faculty of Pharmacy, University of Porto, Rua de Jorge Viterbo Ferreira nº 228, 4050-313 Porto, Portugal*

[b] *Department of Chemistry, University of Warsaw, Pasteura 1, 02-093 Warsaw, Poland*

* Authors for correspondence

E-mail: dsmribeiro@gmail.com

E-mail: joaolms@ff.up.pt

Abstract

In this study an automated flow-based methodology for the fluorometric determination of sulphide, was reported. It relies on the utilization of CdTe nanocrystals as photoluminescent probes, which upon reaction with S^{2-} are subject to a noteworthy concentration-related photoluminescence decrease. The Stern-Volmer plot revealed that for lower S^{2-} concentrations the photoluminescence quenching was based on dynamic processes while for higher concentrations the quenching mechanism was ascribed to the depassivation of the surface ligands, replaced by S^{2-}, resulting in the aggregation of QDs.

The developed approach was automated by resorting to a pulsed stream multi-pumping flow system guaranteeing a high versatility in terms of sample and reagents manipulation and reaction zone formation. Selectivity was assured by means of the utilization of a gas-diffusion unit relying on a hydrophobic PTFE membrane that facilitated sulphide isolation from sample matrix interferences.

Under optimal conditions, a good linear relationship between the photoluminescence quenching magnitude (ΔF) and the logarithmic of S^{2-} concentration within the range 0.25 - 5.0 mmol L^{-1}, was verified (R = 0.998, n = 5). The limit of detection (LOD) was found to be 0.19 mmol L^{-1}. The sampling rate was of about 13 h^{-1}.

Keywords: multi-pumping flow system; gas-diffusion unit; CdTe quantum dots; photoluminescence quenching.

1. Introduction

Semiconductor nanocrystals or quantum dots (QDs) were the subject of intensive research over the last two decades due to their remarkable optical, chemical and electronic properties that make them valuable tools in an ever-increasing range of applications. These highly photoluminescent nanomaterials are particularly useful in chemical analysis where they could replace advantageously the traditional organic fluorophores [1, 2]. By virtue of high quantum yields (QY), broad absorption profiles, narrow, symmetric and tunable emission spectra, long photoluminescent lifetimes, high photobleaching threshold and excellent photochemical stability, QDs exhibited high analytical functionality that could be further improved by the manipulation of their surface chemistry. Throughout the utilization of specific capping ligands it is possible not only to assure aqueous dispersion stability but also to adjust QDs reactivity for a target analyte, by modulating the surface interactions that the QDs could establish [3, 4], which could be exploited for analytical purposes. As a consequence of these surface interactions, mostly with small molecules and ionic species, impressive changes in the physical and chemical properties of the nanoparticles could take place, shaping the photoluminescence emission of the QDs either by enhancing [5-9] or quenching [1, 3, 4, 10-14] its intensity. In what concerns the photoluminescence quenching mechanisms, they generally involve non-radioactive recombination pathways, inner filter effects, electron transfer process and binding interaction[10, 15, 16]. The quenching phenomena can be also dependent of the quencher and QDs nature [13].

Hitherto distinct QDs-based sensors have been developed as photoluminescent probes for ionic species determination, although most were applied with cations and not many

have dealt with the selective determination of anions [12, 17, 18], despite of their fundamental role in many chemical, biological, environmental and industrial processes [19, 20].

The monitoring of sulphide ion in environmental samples, such as waste and hydrothermal waters, as well as, in wine and/or other fermented beverages has a significant importance in order to avoid the highly toxic effects of hydrogen sulphide [21-23]. In fact, hydrogen sulphide (H_2S) is a poisonous gas generally formed in anoxic waters by heterotrophic, sulphate-reducing bacteria and as a result of geochemical processes in hydrothermal systems [20]. Additionally, H_2S has been associated with off-flavors in some alcoholic beverages, resulting from yeast metabolism during the fermentation, which constitutes one of the main concerns on the quality control of wine, beer and other fermented beverages [24]. Therefore, considering the harmful effects of H_2S in human health, environment and industrial production quality, a wide range of analytical methodologies have been developed in order to monitor the level of sulphide ions in different type of samples. These analytical methodologies involve spectrophotometry [25-28], fluorometry [20, 29-34], electrochemical methods [35-38], HPLC [39, 40], gas chromatography [41, 42] , ion chromatography [43] and capillary electrophoresis [44]. In addition, distinct continuous flow methodologies resorting to a variety of detection techniques were also proposed, including fluorometric [45], spectrophotometric [46], chemiluminometric [22] and electrochemical [47] detection.

In this work we have put together the versatility exhibited by multi-pumping flow system (MPFS) [48], in terms of sample and reagents manipulation and facility of reaction zone implementation, and the worthwhile optical properties of CdTe QDs to implement a straightforward methodology for sulphide determination. This combined the sensitivity of the interaction between S^{2-} ion and CdTe QDs and the selectivity

conferred by an in-line separation technique based on a gas-diffusion unit (GDU). The coupling of GDU to MPFS allows isolating the target analyte from interfering species of a highly complex sample matrix, without any additional pre-treatment, resulting in an enhanced selectivity.

The proposed analytical methodology involved the conversion of S^{2-} ion into its gaseous form (H_2S), which diffused from the donor sample stream through a PTFE (Polytetrafluoroethylene) semi-permeable membrane into the MPA-CdTe QDs acceptor stream, yielding a quenching of the nanoparticles photoluminescence. The developed methodology was validated by applying it to the determination of S^{2-} ion in white wine and hydrothermal water samples.

2. Experimental

2.1 Apparatus

For photoluminescence measurement a FP-2020/2025 spectrofluorometer Jasco (Easton, MD, USA), equipped with a 16 μL internal volume flow cell was used (λ_{ex}= 400 nm, λ_{em}=565 nm).

The designed flow manifold comprised four solenoid actuated micropumps (model 120SP, Bio-Chem Valve Inc. Boonton, NJ, USA), which were of the fixed displacement diaphragm type, delivering 10 μL stroke volume.

All connections, illustrated in Figure 1, were made of polytetrafluoroethylene PTFE (Omnifit, Cambridge, UK) material, with 0.8 mm of internal diameter. Lab-made end-fittings, connectors and acrylic confluence points were also used.

A gas diffusion unit, of the sandwich type, was equipped with a hydrophobic gas permeable membrane made of PTFE commercial tape that was positioned between the two channels (donor and acceptor) in order to promote the transfer of gaseous and volatile compounds.

The control of the analytical system was accomplished by means of a microcomputer with software developed using Microsoft Visual Basic 6.0®. The solenoid devices were activated by a homemade power drive based on the ULN2003 chip controlled through communication by the computer parallel port.

QDs absorption and emission spectra were carried out with a Jasco V-660 spectrophotometer (Easton, MD, USA) and a model LS-50B Perkin Elmer luminescence spectrometer (Waltham, MA, USA), respectively. A ThermoElectron Jouan BR4I refrigerated centrifuge (Waltham MA, USA) was used for the separation of the precipitated QDs.

For photoluminescence lifetime measurements a Fluorolog Tau-3 Lifetime spectrofluorimeter (Horiba Jobin Yvon, NJ, USA) was used. The photoluminescence emission was detected with a 90° scattering geometry. All measurements were made using Ludox as a reference standard (τ = 0.00 ns).

The zeta potential of the nanocrystals was obtained using a BI-MAS Dynamic light scattering (DLS) instrument (Brookhaven Instruments, USA).

The morphology of the nanoparticles was observed by transmission electron microscopy (TEM) using an electron microscope JEOL JEM 1400 TEM (Tokyo, Japan), at an acceleration voltage of 100 kV, equipped with a Gatan SC 1000 ORIUS CCD camera (Warrendale, PA, USA).

2.2 Samples, standards and reagents

All solutions were prepared with water from a Milli-Q system (specific conductivity ≤ 0.1 μS cm^{-1}) and chemicals were of analytical reagent grade quality. Reagents were not subjected to any further purification.

Several QDs solutions were tested by using phosphate and borate buffers, adjusted to different pH within the range of 8-12. For the assays, a aqueous dispersion containing 0.50 μmol L^{-1} of CdTe QDs was daily prepared by dissolving 6.10 mg of the synthesized and purified CdTe QDs, with a size of 3.01 nm, in 25 mL of phosphate buffer pH=11.

The sulphide stock solution (0.05 mol L^{-1}) was prepared by dissolving 97.55 mg of Na_2S (Sigma-Aldrich, St. Louis MO, USA) in 25.0 mL volumetric flask, using 0.05 mol L^{-1} NaOH as solvent. Due to sulphide instability, the final solution was daily standardized iodimetrically. Working standard solutions (0.250–5.0 mmol L^{-1}) were daily prepared from the previous solution by rigorous dilution of selected aliquots (0.125 –2.5 mL) in a series of 25.0 mL volumetric flasks, the final volume being completed with 0.05 mol L^{-1} NaOH.

For the preliminary studies, a 0.05 mol L^{-1} sodium sulphite stock solution was prepared by dissolving 157.55 mg of Na_2SO_3 (Merck, Darmstadt, Germany) in 25 mL of water. Sulphite standard solutions were prepared by appropriate dilution of the stock solution in 25.0 mL of water.

A 0.05 mol L^{-1} NaOH and 0.75 mol L^{-1} HCl solutions were used as acceptor and sample conditioning streams, respectively.

Six commercially wine samples, obtained from local markets and seven hydrothermal waters samples, collected in different hot springs of Portugal, were analysed according

to the developed method. All samples were alkalinized with NaOH 0.05 mol L^{-1} before insertion into the flow system.

For the synthesis of the CdTe quantum dots, tellurium powder (200 mesh, 99.8%), sodium borohydride ($NaBH_4$, 99%), cadmium chloride hemi(pentahydrate) ($CdCl_2 \cdot 2.5H2O$, 99%) were purchased from Sigma–Aldrich (St. Louis, MO, USA); 3-mercaptopropionic acid (MPA, 99%) and absolute ethanol (99.5%) were obtained from Fluka (St. Louis MO, USA) and Panreac (Barcelona, Spain) respectively.

2.3 Synthesis of CdTe quantum dots

Three different diameters of MPA-capped CdTe QDs were synthesized as described by Silvestre *et al.* [49] with some modifications. Briefly, the first stage consists on the reduction of tellurium with $NaBH_4$ in N_2 saturated water to produce NaHTe. After all tellurium has been completely consumed the resulting solution was transferred to another flask containing 4.0×10^{-3} mol of $CdCl_2$ and 6.8×10^{-3} mol of MPA in 100 mL N_2 saturated solution. The pH of the solution was adjusted to 11.5 by the addition of 1.0 mol L^{-1} NaOH solution. The molar ratio of Cd^{2+}:Te^{2-}:MPA was fixed at 1:0.1:1.7. The size of CdTe QDs was tuned by varying the refluxing time.

In order to remove the contaminants, purification of CdTe QDs was conducted by precipitation in absolute ethanol and the precipitate was subsequently separated by centrifugation, vacuum dried, kept in amber flasks and protected from light, for posterior use.

2.4 Manifold and MPFS procedure

The analytical flow manifold devised for fluorometric monitoring of sulphide in white wines and hydrothermal waters is pictured in Figure 1. Due to the relatively complex composition of wine samples and the high reactivity of QDs, which somehow restrained selectivity, the developed flow system was implemented in a configuration that aimed at simultaneously enhance the selectivity and suppress the possible interfering effect from the sample matrix on the QDs photoluminescence intensity. In addition, it sought high sensitivity without compromising the sampling rate. With this purpose, in the outset of the analytical flow manifold was paid special attention to the inclusion of an in-line chemical separation stage carried out through the incorporation of a gas diffusion unit, which allowed the isolation of the analyte, in its gaseous form, from the sample matrix. Thus, the analytical flow system employed four solenoid micro-pumps (P_1-P_4) which were responsible for the individual handling of sample and reagent solutions. At the beginning of each analytical cycle, all flow tubing was filled with the corresponding solutions, by activating the respective micro-pump. P_1, P_2 and P_4 were responsible for inserting and propelling the sample, HCl (donor stream) and QDs solutions, respectively, whilst micro-pump P_3 was responsible for the propulsion of the acceptor stream (NaOH) towards detection, establishing the baseline.

The developed analytical cycle started with the combined insertion of a pre-set number of sample pulses and HCl solutions in confluence point X_1, exploiting the merging zones approach, by the simultaneous actuation of micro-pumps P_1 and P_2, at a fixed pulse time of 0.25 s. This step allowed the acidification of the sample and the conversion of S^{2-} initially present in the sample into volatile chemical species (H_2S). By actuating P_1 and P_2, and keeping P_3 deactivated, this first reaction zone was directed

towards the gas diffusion unit and the gaseous species permeate through the Teflon membrane towards the acceptor stream, while the sample matrix was sent to waste. The effect of the alkalinity of the acceptor solution promoted the reconversion of the gaseous species into S^{2-}. Then, by simultaneous actuation of micro-pumps P_3 and P_4 (P_1 and P_2 deactivated), QDs aqueous dispersion and S^{2-} alkaline were mixed at confluence point X_2, establishing a second reaction zone. The reaction zone was then carried towards the detector through the repeated actuation of P_3 (10 μL per stroke), at a fixed pulse time of 0.25 s (corresponding to a pulse frequency of 2.5 Hz, considering the 0.15 s of the micro-pump activation) that enabled establishing a flow rate of 1.50 mL min^{-1}. The photoluminescence emission was monitored at 565 nm (λ_{ex}= 400 nm).

2.5 Characterization of quantum dots

The absorption and photoluminescence spectra of the MPA-capped CdTe QDs synthetized with different refluxing times are shown in Figure 2. The different sized nanocrystals exhibited broad absorption with a well-defined maximum for the first excitonic transition and narrow and symmetric emission spectra with Full Width at Half Maximum (FWHM) values ranging between 43.29 to 45.69 nm. These FWHM values demonstrated that as-prepared MPA-CdTe QDs are nearly monodisperse and homogeneous.

According to the experimental model proposed by Yu *et al.* [50], the CdTe nanoparticles sizes were estimated using equation 1, where D is the QD diameter (nm) and λ (nm) the wavelength corresponding to the maximum absorbance of the first transition.

$$D = (9.8127 \times 10^{-7})\lambda^3 - (1.7147 \times 10^{-3})\lambda^2 + (1.0064)\lambda - (194.84) \quad \text{(Equation 1)}$$

For the QDs synthesized in our work, the estimated diameter were about 1.36, 1.98 and 3.01 nm wherein the maximum absorption wavelengths were recorded at 472, 488 and 532 nm (Figure 2 (A)).

In order to corroborate the results obtained by spectrophotometric and fluorometric methods, the morphology and the particle size of the 3.01 nm MPA-CdTe QDs were studied by transmission electron microscopy (TEM). The TEM image confirmed that the QDs have the average size around 3 nm, also demonstrating the formation of well dispersed nanoparticles with almost spherical shape.

With the aim of standardize the preparation of CdTe QDs solutions, the molar concentration of the different sized nanocrystals was determined by establishing firstly the molar absorptivity (ε) using the equation 2, in which ΔE is the transition energy corresponding to the first absorption peak expressed in eV.

$$\varepsilon = 3450\Delta E(D)^{2.4} \qquad \text{(Equation 2)}$$

By knowing the ε value and the absorbance of a known mass concentration solution, the molar concentration was estimated by applying the Lambert-Beer's Law.

3. Results and Discussion

Preliminary batch experiments showed that in the presence of sulphide CdTe quantum dots capped with different ligands, in particular those passivated with 3-mercaptopropionic acid and glutathione exhibited a pronounced photoluminescence

quenching. However, the glutathione-capped ones were also subject to interference from other ionic species, such as sulphite, which hindered their analytical usefulness.

3.1 Preliminary assays

Steady-state photoluminescence measurements were performed aiming to evaluate the influence of the sulphide anion on the photoluminescence properties of the synthetized MPA-CdTe QDs. These preliminary assays involved the preparation of several solutions containing 0.5 μmol L^{-1} of QDs and increasing concentrations of Na_2S within a range of 0 – 0.5, 0 – 1.0 and 0 – 2.0 mmol L^{-1} for nanoparticles sizes of 1.36, 1.98 and 3.01 nm, respectively. The photoluminescence emission spectra of the different prepared solutions were monitored for wavelengths comprised between 450 nm and 650 nm upon excitation at 400 nm.

The obtained results, depicted in Figure 3, revealed that by adding increasing concentrations of S^{2-} ion the photoluminescence intensity of the QDs was significantly quenched. Additionally, it was observed (Figure 3 A)) that increasing the QDs diameter it was required to add higher S^{2-} concentrations in order to obtain the same quenching effect on the photoluminescence emission of the nanocrystals. Beyond the quenching effect of sulphide on the photoluminescence intensity of QDs, a redshift of the wavelength of maximum emission was also observed, which was more noticeable for the smaller nanoparticles. In fact, for the 1.36 nm QDs, the redshift of the photoluminescence emission peak was observed immediately upon the addition of 0.125 mmol L^{-1} of sodium sulphide whilst for the bigger QDs the redshift effect occurs only upon the addition of higher S^{2-} concentrations, namely 0.300 mmol L^{-1} and 1.75 mmol L^{-1} for the QDs sizes of 1.98 and 3.01 nm, respectively.

With the aim of investigating a possible occurrence of redshift effect in the wavelength corresponding to the maximum absorbance of the first electronic transition, the absorbance spectra of the different solutions above prepared were obtained.

As shown in Figure 4, a redshift of the wavelength of maximum absorbance was observed for the QDs with 1.36 nm upon the first addition of S^{2-} anion with a concentration of 0.125 mmol L^{-1} while for the bigger QDs this phenomenon occurs after the addition of higher sulphide concentrations which were in accordance with the respective photoluminescence spectra.

Taking into account the presence of possible interferences in the determination of sulphides in wines by the developed methodology, the study of the influence of sulphites on the photoluminescence of QDs was performed. As it happened with the assays of the influence of sulphide anion on the luminescence properties of QDs, the interaction between sulphite ion and QDs was also studied by replacing the concentrations of Na_2S by equimolar Na_2SO_3 solutions. The results obtained for the different sized QDs revealed that there was no significant influence of SO_3^{2-} ion on the luminescence properties of the nanoparticles since no change in photoluminescence intensity neither no shift of the wavelength of maximum emission was observed.

3.2 Quenching mechanism of MPA-CdTe QDs upon interaction with sulphide anion

According to the literature, for the main two florescence quenching ways, namely dynamic and static quenching, the dependence of the photoluminescence intensity (F_0/F) upon the quencher concentration is linear and both are described by the Stern-Volmer equation:

$$F_0/F = 1 + K_{SV}[Q] \quad \text{(Equation 3)}$$

$$F_0/F = 1 + K[Q] \quad \text{(Equation 4)}$$

wherein F_0 and F are the photoluminescence intensity in the absence and presence of the quencher, respectively; Q is the quencher concentration; K_{SV} and K are the Stern-Volmer quenching constant (dynamic quenching) and the association constant (static quenching), respectively. Thus, photoluminescence intensity data obtained in preliminary assays for the interaction between S^{2-} and 3.01 nm MPA-CdTe QDs were then analysed according to Stern–Volmer quenching theory being the corresponding Stern-Volmer plot depicted in Figure 5. As it can be seen in Figure 5, the Stern-Volmer plot is an upward curvature instead of a straight line being the modified form of the Stern–Volmer equation of third order which was described as following:

$$F_0/F = 47.418\,[S^{2-}]^3 - 46.341[S^{2-}]^2 + 12.261[S^{2-}] + 0.7538, (R = 0.9999) \quad \text{(Equation 5)}$$

The characteristic feature of the Stern-Volmer plot revealed that the photoluminescence of QDs can be quenched with S^{2-} ion by various effects, namely, dynamic and static processes. For low S^{2-} concentrations, a linear Stern–Volmer relationship between F_0/F and [Q] was verified. So, to better understand what kind of photoluminescence quenching occur for these concentration values, photoluminescence lifetime measurements of a 0.5 μmol L^{-1} of 3.01 nm QDs in absence and in presence of increasing S^{2-} concentrations were performed. As can be seen in Table 1, the increase of sulphide concentration causes a decrease in the photoluminescence lifetime of the QDs.

This demonstrates that, at these concentration values the quenching mechanism was based on the dynamic processes. For high S^{2-} concentrations the plot changed into an upward curvature, concave towards the y-axis. This change may have occurred due to the aggregation of QDs, resulting from the depassivation of the surface ligands, replaced by S^{2-}, which decreased the QDs stability in aqueous solution. This loss of the stabilizing layer leads to a strong photoluminescence quenching of MPA-CdTe QDs and the consequent aggregation of nanoparticles contributes to the observed red-shift effect in the absorption and emission spectra [13, 51]. The QDs instability in aqueous dispersion and the increased tendency to aggregate was proved through the zeta potential measurements of two different solutions, containing: (i) 0.5 μmol L^{-1} CdTe QDs (3.01 nm) and (ii) a mixture of 0.5 μmol L^{-1} of the QDs (3.01 nm) and 1.0 mmol L^{-1} of S^{2-}. Aiming to eliminate the excess of free sulphide, the solutions were precipitated with ethanol, centrifuged and re-dissolved with deionized water. The zeta potential of the QDs aqueous dispersion was -44.38 ± 1.29 mV and that of the mixture of QDs and sulphide anion was -27.36 ± 1.33 mV. As the absolute values of zeta potential decreased in the presence of the S^{2-}, alterations on the QDs surface charges was demonstrated and consequently the tendency to aggregate, diminishing thus their stability in aqueous dispersion.

3.3 Optimization of the MPFS

Considering the influence of sulphide anion on the photoluminescence of MPA-CdTe nanoparticles, it was developed a simple and fast QDs-based analytical methodology for the selective determination of sulphide in white wines and hydrothermal waters. The analytical methodology was implemented in a micro-flow system, exploiting the multi-

pumping flow concept, which was coupled with an in-line gas diffusion unit. With the purpose to optimize the efficiency of the in-line chemical separation of S^{2-} from the matrix and, at same time, in order to obtain a better compromise between sensitivity, reagent consumption, detection limit and sampling rate, optimization studies of the physical and chemical parameters were performed. In the optimization studies and real samples analysis the calibration curves were established between the photoluminesce quenching magnitude and the logarithmic of S^{2-} concentration. The ΔF was the ratio between the difference of the QDs photoluminescence in absence (F_0) and in presence of the quencher (F), which was calculated according to the equation 6:

$$\Delta F = (F_0 - F)/F_0 \times 100 \quad \text{(Equation 6)}$$

3.3.1 Influence of MPA-CdTe QDs sizes and molar concentration

The influence in the analytical signal of the 3 different sized QDs (1.36, 1.98 and 3.01 nm) at three QDs concentrations values, namely 0.25, 0.5 and 1.0 μmol L^{-1}, were evaluated.

These studies were carried out using QDs volume of 50 μL (5 pulses), 0.025 mol L^{-1} of NaOH as acceptor stream, 0.5 mol L^{-1} of HCl as donor stream and a reactor coil length of 50 cm. For each size and concentration of QDs tested, calibration curves with different sulphide standards solutions (0.0 – 30.0 mmol L^{-1}) were established being the results analysed resorting to a comparison between the obtained slopes.

The results demonstrated that by increasing QDs diameter the magnitude of the analytical signal also increased, indicating that the nanoparticles of bigger size exhibited higher quantum yield. Thus, the 3.01 nm QDs, with higher QY, was selected for further

assays since the quantification of S^{2-} contents in real samples was based on the inhibition of photoluminescence signal (PL quenching). The QDs concentration revealed a noteworthy influence on the sensitivity of the analytical methodology. It was possible to see a sensitivity increase of about 11 and 21% when using the QDs concentration of 0.50 μmol L^{-1} in comparison with 0.25 and 1.0 μmol L^{-1}, respectively. For the succeeding optimization assays the QDs concentration of 0.50 μmol L^{-1} was selected.

3.3.2 Influence of chemical composition of donor and acceptor streams

The chemical composition of the donor and acceptor streams could affect the performance of the in-line chemical separation technique. Therefore, one of the key conditions for an efficient performance of the gas-diffusion MPFS system was the pre-mixture of the sample with an acidic solution for the conversion of sulphide anion into a volatile compound (H_2S). Indeed, the extension of S^{2-} in H_2S conversion was dependent on the HCl concentration. Additionally, an alkaline solution (NaOH) had to be used as acceptor stream for the reconversion of H_2S to S^{2-}. The NaOH concentration can play an important role in H_2S diffusion through the PTFE membrane.

Thus, the influence of HCl and NaOH concentration on the sensitivity of the method was assessed over a concentration range from 0.10 to 1.0 mol L^{-1} and 0.010 to 0.10 mol L^{-1}, respectively. The study of the influence of HCl concentration was performed using a set of sulphide standard solutions (0 – 30.0 mmol L^{-1}) and fixing the concentration of NaOH at 0.025 mol L^{-1}. For each HCl concentration tested, calibration curves were established for the evaluation of the sensitivity through the analysis of the obtained slopes. The results (Figure 6A) showed a more pronounced increase of sensitivity for

HCl concentrations from 0.10 up to 0.75 mol L^{-1}, and for higher concentrations the increase was less pronounced. Therefore, a donor stream composed by 0.75 mol L^{-1} of HCl was chosen for posterior optimization studies.

Similarly, the study of the influence of NaOH concentration was conducted using the same sulphide standard solutions and fixing the HCl concentration at 0.75 mol L^{-1}. As perceived by the results (Figure 6B) the sensitivity markedly increased with the NaOH concentration up to 0.050 mol L^{-1}, tending to stabilization for higher concentration values. Then, a NaOH solution with a concentration of 0.050 mol L^{-1} was selected as acceptor stream for further assays.

3.3.3 Influence of pH conditions

The influence of different pH buffer solutions on the sensitivity of the method was assayed in a range between 8.0 and 12.0, by using phosphate and borate buffers. The results achieved from this study (Figure 7) demonstrated that for pH values ranging 8 and 10 no significant variations on the sensitivity was observed. By increasing pH values from 10 to 11 a noteworthy increase was verified and for higher pH values the sensitivity slightly decreased. So, a pH of 11 was chosen for the posterior experiments.

3.3.4 Influence of physical flow parameters

The dispersion phenomenon of the reaction zone and the reaction development of the interaction between S^{2-} and QDs are determined by the operational flow systems parameters. The following experiments were performed aiming to study and optimize some physical parameters, namely, the reactor length, QDs volume and the flow rate of

the reaction zone stream towards to the detector, in order to yield an adequate reaction development and dispersion level inside the system, maximizing thus the sensitivity of the method.

The study of the influence of the QDs volume and the reactor length was simultaneously conducted. For each reactor's length studied, specifically 20, 50, 75 and 100 cm, the number of QD pulses varied between 3 and 11 which correspond to volumes between 30 and 110 μL. Additionally, for all reactor's length and QD volumes tested, calibration curves were established for S^{2-} concentrations between 1.0 to 30.0 mmol L^{-1}. The results revealed (Figure 8) that the higher the reactor's length the higher the sensitivity of the methodology. In opposition, for minor QDs volumes a higher sensitivity of the methodology was achieved. Moreover, for higher reactor's length and minor QD volumes it was necessary decrease the working concentrations of sulphide (0.50 – 5.0 mmol L^{-1}) with the purpose of obtaining a linear relationship between the photoluminescence quenching percentage (ΔF(%)) and the logarithmic of S^{2-} concentration, and, as a consequence, the detection limit also decreased. These last obtained results indicated that the interaction of sulphide anion with MPA-CdTe QDs had a low reaction rate. Indeed, the use of a long reactor combined with a low QDs volume leads to more adequate reaction zone dispersion and consequently an improved reaction development enabling to obtain a higher sensitivity of the methodology. Therefore, for the posterior assays a reactor length of 100 cm and 30 μL of QDs (corresponding to 3 pulses) were selected.

Another relevant parameter in flow manifold was the flow rate which is determined by the micro-pumps pulse times and can affect not only the reaction development but also the sampling rate. In this optimization assay, for different flow rates of 2.18, 1.50, 1.09 and 0.80 mL min^{-1} (corresponding to pulse times of 0.125, 0.25, 0.40 and 0.60 s) used

to transport the reaction zone to the detector, calibration curves for sulphide concentrations ranging from 0.25 to 5.0 mmol L^{-1} were obtained. According to the obtained results (Figure 9), the sensitivity of the methodology increased by varying the flow rate from 0.80 to1.50 mL min^{-1} and then, slightly decreased for higher values. Aiming at a compromise between sensitivity and sampling rate, a flow rate of 1.50 mL min^{-1} (corresponding to pulse times of 0.25 s) was selected.

3.4 Method validation

Under the optimal chemical and physical conditions previously established a linear relationship between the photoluminescence quenching magnitude and the logarithmic of S^{2-} concentration in the range of 0.25 - 5.0 mmol L^{-1} was obtained. Therefore, the analytical curve was represented by the equation (Eq. (7)):

$$\Delta F = 61(\pm 2) \times \text{Log } C + 233(\pm 7) \quad \text{(Equation 7)}$$

in which ΔF was the photoluminescence quenching, expressed in percentage and C was the S^{2-} concentration, with a correlation coefficient of 0.998 (n = 5). The detection limit calculated from the equation of the calibration curve[52] was about 0.19 mmol L^{-1}.

The accuracy of the proposed GD-MPFS was evaluated by monitoring the S^{2-} in hydrothermal waters, collected in different hot springs of Portugal, and the obtained results were compared with those furnished by the reference procedure recommended by Standard Methods Committee[53]. The reference method involved an iodometric titration under acidic conditions. The obtained results compiled in the Table 2 showed a

good agreement between both procedures with relative deviations between -2.57 and 3.24%. Moreover, the results were statistically compared in terms of accuracy and precision by using the Student's t-test and variance ratio F-test. With respect to accuracy the paired Student's t-test confirmed that there were no significant difference between the proposed and reference methodologies for a confidence level of 95% since the calculated value of t (0.796) was lower than the critical tabulated value (t = 2.447). Additionally by comparing the methodologies regarding the precision, the application of variance ratio F-test allowed to observe that there were no significant differences between the results obtained by both procedures ($F_{calculated}$ = 1.17, $F_{tabulated}$ = 4.28).

The precision of the proposed methodology was estimated through the repeated analysis of each sample solution (3 determinations for each sample), which revealed a good repeatability taking into account the calculated concentration ranges for a confidence level of 95%.

The proposed methodology allowed a determination rate of about 52 h^{-1}, equivalent to the analysis of about 13 samples per hour (considering the time required for sample replacement).

Considering the obtained recovery values (Table 2), ranging from 96.4 to 108.0%, for the determination of S^{2-} in waters samples spiked with two different concentrations of the analyte (0.50 and 2.0 mmol L^{-1}), the good selectivity of the proposed method was demonstrated.

However, in order to evaluate the selectivity of the method in the analysis of samples with a more complex matrix, the chemical monitoring of S^{2-} in white wines commercially available in the Portuguese market were performed by spiking the samples with 0.5 and 2.0 mmol L^{-1} of sulphide ion. The obtained results, summarized in Table 3, confirmed the good selectivity of the proposed method for the analysis of S^{2-} in

samples with complex matrices taking into account the recovery values ranging from 96.0 to 106.3%. It should be noticed that the detection limit of the developed methodology was too high to allow the direct determination of sulphide in white wine samples. However the selectivity that it evidences, significantly higher than that was provided by alternative methods, ensures that it could be used in the chemical control of the high sulphide levels that occur during the white wine production stage.

The selectivity of the proposed methodology was mostly guaranteed by gas diffusion unit, which is responsible for isolating the analyte from the sample matrix avoiding possible interferences of others compounds commonly present in wine and hydrothermal waters. As only volatile compounds could permeate the membrane, the SO_3^{2-} ion could be a possible interferent. However, preliminary assays demonstrated that sulphite had no influence on the QDs photoluminescence properties.

In comparison with other flow-based procedures [22, 45-47] found in literature the proposed methodology exhibits a higher detection limit but, at the same time, it enables the carrying out of the analysis at an increased sampling rate. Moreover, it affords a wider linear working range. This latter aspect is very important in the determination of S^{2-} in hot spring waters because these exhibit extremely variable sulphide levels (usually high) and thus it is possible to analyse a wide range of unknown concentrations with a single calibration step and without the need for any sample dilution.

4. Conclusions

The study of the interaction between sulphide and QDs revealed that the anion specie effectively quenched the photoluminescence intensity of the nanoparticles causing, at same time, a redshift of the wavelength of maximum emission and also in the

wavelength corresponding to the maximum absorbance of the first electronic transition. The redshift effect observed was more pronounced for smaller nanocrystals.

A carefully investigation revealed that the quenching process involved both dynamic and static mechanisms depending on the concentration of sulphide ion added. Indeed, for lower S^{2-} concentrations the photoluminescence quenching was based on dynamic processes since the QD lifetime varied proportionally with the concentration of S^{2-} ion. For higher sulphide concentrations the quenching mechanism was probably attributed to the depassivation of the surface ligands, replaced by S^{2-}, resulting in the aggregation of QDs which was confirmed by zeta potential measurements.

Also, it was demonstrated that advantages characteristics of multi-pumping flow system, such as a great flexibility in handling solutions and a strict and reproducible control of the reaction conditions, could be further emphasised if combined with the sensitivity afforded by MPA-CdTe QDs and the high selectivity granted by the gas-diffusion module. This synergy was favourably exploited in the determination of sulphide ion in white wine and hydrothermal water samples.

Taking into account the sensitivity, selectivity, accuracy and precision, the proposed methodology could be considered as a valuable analytical tool easily adaptable for routine environmental analysis of samples with complex matrices and also in the industry process control of sulphide ion during wine production.

Acknowledgements

S. Sofia M. Rodrigues thanks the “Fundação para a Ciência e Tecnologia” and FSE (Quadro Comunitário de Apoio) for the Ph.D. grant (SFRH/BD/70444/2010). This work received financial support from the European Union (FEDER funds through

COMPETE) and National Funds (FCT, Fundação para a Ciência e Tecnologia) through project Pest-C/EQB/LA0006/2013. The work also received financial support from the European Union (FEDER funds) under the framework of QREN through Project NORTE-07-0124-FEDER-000067. To all financing sources the authors are greatly indebted.

References

1. O. Adegoke, E. Hosten, C. McCleland and T. Nyokong, *Anal. Chim. Acta*, 2012, **721**, 154-161.
2. C. Frigerio, D. S. M. Ribeiro, S. S. M. Rodrigues, V. L. R. G. Abreu, J. A. C. Barbosa, J. A. V. Prior, K. L. Marques and J. L. M. Santos, *Anal. Chim. Acta*, 2012, **735**, 9-22.
3. W. Zhong, J. Liang and J. Yu, *Spectrochim. Acta A*, 2009, **74**, 603-606.
4. T. T. Gan, Y. J. Zhang, N. J. Zhao, X. Xiao, G. F. Yin, S. H. Yu, H. B. Wang, J. B. Duan, C. Y. Shi and W. Q. Liu, *Spectrochim. Acta A*, 2012, **99**, 62-68.
5. N. Myung, Y. Bae and A. J. Bard, *Nano Lett.*, 2003, **3**, 747-749.
6. Q. Wang, Y. Kuo, Y. Wang, G. Shin, C. Ruengruglikit and Q. Huang, *J. Phys. Chem. B*, 2006, **110**, 16860-16866.
7. C. Frigerio, V. L. R. G. Abreu and J. L. M. Santos, *Talanta*, 2012, **96**, 55-61.
8. Z. Liu, S. Liu, P. Yin and Y. He, *Anal. Chim. Acta*, 2012, **745**, 78-84.
9. G. L. Wang, H. J. Jiao, X. Y. Zhu, Y. M. Dong and Z. J. Li, *Talanta*, 2012, **93**, 398-403.
10. C. Bo and Z. Ping, *Anal. Bioanal. Chem.*, 2005, **381**, 986-992.
11. C. L. Wu and Y. B. Zhao, *Anal. Bioanal. Chem.*, 2007, **388**, 717-722.
12. C.-R. Tang, Z.-h. Su, B.-G. Lin, H.-W. Huang, Y.-L. Zeng, S. Li, H. Huang, Y.-J. Wang, C.-X. Li, G.-L. Shen and R.-Q. Yu, *Anal. Chim. Acta*, 2010, **678**, 203-207.
13. K. Santhosh, S. Patra, S. Soumya, D. C. Khara and A. Samanta, *Chemphyschem*, 2011, **12**, 2735-2741.
14. Z. Cai, B. Shi, L. Zhao and M. Ma, *Spectrochim. Acta A*, 2012, **97**, 909-914.

15. Y. Chen and Z. Rosenzweig, *Anal. Chem.*, 2002, **74**, 5132-5138.

16. S. S. M. Rodrigues, A. S. Lima, L. S. G. Teixeira, M. d. G. A. Korn and J. L. M. Santos, *Fuel*, 2014, **117, Part A**, 520-527.

17. W. J. Jin, J. M. Costa-Fernández, R. Pereiro and A. Sanz-Medel, *Anal. Chim. Acta*, 2004, **522**, 1-8.

18. W. J. Jin, M. T. Fernandez-Arguelles, J. M. Costa-Fernandez, R. Pereiro and A. Sanz-Medel, *Chem. Commun.*, 2005, 883-885.

19. R. Martinez-Manez and F. Sancenon, *Chem. Rev.*, 2003, **103**, 4419-4476.

20. H. R. Rajabi, M. Shamsipur, A. A. Khosravi, O. Khani and M. H. Yousefi, *Spectrochim. Acta A*, 2013, **107**, 256-262.

21. L. Ferrer, G. de Armas, M. Miro, J. M. Estela and V. Cerda, *Analyst*, 2005, **130**, 644-651.

22. F. Maya, J. M. Estela and V. Cerdà, *Anal. Chim. Acta*, 2007, **601**, 87-94.

23. K. J. Wallace, S. R. Cordero, C. P. Tan, V. M. Lynch and E. V. Anslyn, *Sensor. Actuat. B - Chem.*, 2007, **120**, 362-367.

24. M. Ugliano, R. Kolouchova and P. A. Henschke, *J. Ind. Microbiol. Biotechnol.*, 2011, **38**, 423-429.

25. S. J. Chen, X. S. Zhang, L. Y. Yu, F. M. Cao, H. H. Zhao and H. Li, *J. Soc. Leather Technol. Chem.*, 2011, **95**, 121-125.

26. L. Tai and Y.-x. Zhou, in *Mechanical and Aerospace Engineering, Pts 1-7*, ed. W. Fan, 2012, vol. 110-116, pp. 3086-3091.

27. M. Ghadiri, H.-R. Kariminia and R. R. Azad, *Ecotox. Environ. Safe.*, 2013, **91**, 117-121.

28. J. Bae, M. G. Choi, J. Choi and S.-K. Chang, *Dyes Pigments*, 2013, **99**, 748-752.

29. Holzbech.J and D. E. Ryan, *Anal. Chim. Acta*, 1974, **68**, 458-461.

30. H. Xia, G. Q. Gong and H. G. Wang, *Bull. Soc. Chim. Belg.*, 1996, **105**, 5-8.

31. M. M. F. Choi, *Analyst*, 1998, **123**, 1631-1634.

32. B.-H. Zhang, F.-Y. Wu, Y.-M. Wu and X.-S. Zhan, *J. Fluoresc.*, 2010, **20**, 243-250.

33. J. F. da Silveira Petruci and A. A. Cardoso, *Microchem. J.*, 2013, **106**, 368-372.

34. A. Punta, F. J. Barragan, M. Ternero and A. Guiraum, *Analyst*, 1990, **115**, 1499-1503.

35. D. Giovanelli, N. S. Lawrence, L. Jiang, T. G. J. Jones and R. G. Compton, *Analyst*, 2003, **128**, 173-177.

36. T. V. Titova, N. S. Borisova and N. F. Zakharchuk, *Anal. Chim. Acta*, 2009, **653**, 154-160.

37. D. Huang, B. Xu, J. Tang, J. Luo, L. Chen, L. Yang, Z. Yang and S. Bi, *Anal. Methods*, 2010, **2**, 154-158.

38. Y. Dilgin, B. Kizilkaya, B. Ertek, N. Erena and D. G. Dilgin, *Talanta*, 2012, **89**, 490-495.

39. D. Tang and P. H. Santschi, *J. Chromatogr. A*, 2000, **883**, 305-309.

40. J. C. Savage and D. H. Gould, *J. Chromatogr.B*, 1990, **526**, 540-545.

41. N. Ichinose, K. Nakamura and C. Shimizu, *J. Chromatogr. A*, 1984, **292**, 393-401.

42. R. r. Hyšpler, A. Tichá, M. Indrová, Z. Zadák, L. Hyšplerová, J. Gasparič and J. Churáček, *J. Chromatogr. B*, 2002, **770**, 255-259.

43. C. Giuriati, S. Cavalli, A. Gorni, D. Badocco and P. Pastore, *J. Chromatogr. A*, 2004, **1023**, 105-112.

44. K. Fukushi and K. Hiiro, *J. Chromatogr. A*, 1987, **393**, 433-440.

45. M. A. Spaziani, M. Tinani and M. K. Carroll, *Analyst*, 1997, **122**, 1555-1557.

46. G. de Armas, L. Ferrer, M. Miró, J. M. Estela and V. c. Cerdà, *Anal. Chim. Acta*, 2004, **524**, 89-96.

47. Y. Dilgin, S. Canarslan, O. Ayyildiz, B. Ertek and G. Nişli, *Electrochim. Acta*, 2012, **66**, 173-179.

48. R. A. S. Lapa, J. L. F. C. Lima, B. F. Reis, J. L. M. Santos and E. A. G. Zagatto, *Anal. Chim. Acta*, 2002, **466**, 125-132.

49. C. I. Silvestre, C. Frigerio, J. L. Santos and J. L. Lima, *Anal. Chim. Acta*, 2011, **699**, 193-197.

50. W. W. Yu, L. H. Qu, W. Z. Guo and X. G. Peng, *Chem. Mater.*, 2003, **15**, 2854-2860.

51. A. Nag, M. V. Kovalenko, J.-S. Lee, W. Liu, B. Spokoyny and D. V. Talapin, *J. Am. Chem. Soc.*, 2011, **133**, 10612-10620.

52. J. N. Miller and J. C. Miller, *Statistics and Chemometrics for Analytical Chemistry*, 6th edn., Prentice Hall/Pearson, England, 2010.

53. A. P. H. Association, in *Standard Methods for the Examination of Water and Wastewater*, eds. L. S. Clesceri, A. E. Greenberg and A. D. Eaton, Washington DC, 20th edn., 1998, pp. 162-172.

Captions for figures:

Figure 1 – Schematic diagram of the gas diffusion multi-pumping flow system. P_1 – P_4: solenoid micro-pumps (10 µL stroke volumes); X_1 and X_2, confluence points; GDU, gas diffusion unit; DC, donor channel; AC, acceptor channel; RC, 100 cm reactor coil; D, photoluminescence detector; S, sample prepared in 0.050 mol L^{-1} NaOH; DS, donor stream: 0.75 mol L^{-1} HCl; AS, acceptor stream: 0.050 mol L^{-1} NaOH; QDs, 3.01 nm MPA-CdTe quantum dots with 0.50 µmol L^{-1} prepared in phosphate buffer pH = 11; W, waste.

Figure 2 - Normalized UV-vis absorption (A) and photoluminescence (B) spectra of the synthesized MPA-CdTe QDs. Photograph of the QDs solutions at visible light (C) and irradiated with 365 nm light (D).

Figure 3 – A) Influence of the sulphide anion concentration on the luminescence properties of 0.5 µmol L^{-1} MPA-CdTe QDs with different sizes: (♦) 1.36 nm; (■) 1.98 nm and (▲) 3.01 nm. B) Photoluminescence emission spectra of 0.5 µmol L^{-1} MPA-CdTe with a size of (I) 1.36 nm; (II) 1.98 nm; (III) 3.01 nm, in the presence of different S^{2-} concentrations**.**

Figure 4 – Normalized UV-vis absorption spectra of 0.5 µmol L^{-1} MPA-CdTe with a size of (A) 1.36 nm; (B) 1.98 nm; (C) 3.01 nm, in the presence of different S^{2-} concentrations**.**

Figure 5 – Stern-Volmer plot fit curve of the interaction between the 3.01 nm MPA-CdTe QDs and sulphide anion at different concentration levels.

Figure 6 – Influence of (A) HCl and (B) NaOH concentrations on the sensitivity of the methodology.

Figure 7 - Influence of the pH of QDs solutions on the sensitivity of the analytical methodology.

Figure 8 – Influence of the reactor's length and QDs volumes (number of pulses) on the sensitivity of the methodology. (●) 30 µL (3 pulses); (■) 50 µL (5 pulses); (▲) 70 µL (7 pulses); (♦) 90 µL (9 pulses) and (×) 110 µL (11 pulses).

Figure 9 - Influence of the (A) pulse time and (B) the corresponding flow rate on the sensitivity of the methodology.

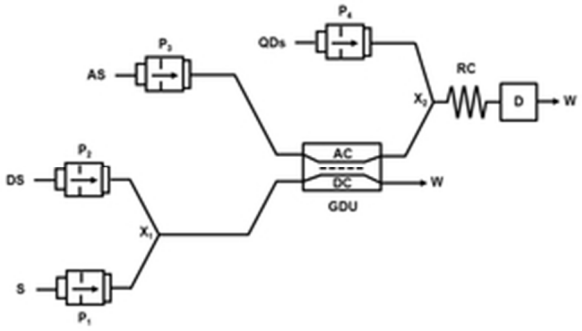

Figure 1 – Schematic diagram of the gas diffusion multi-pumping flow system. P1 – P4: solenoid micro-pumps (10 µL stroke volumes); X1 and X2, confluence points; GDU, gas diffusion unit; DC, donor channel; AC, acceptor channel; RC, 100 cm reactor coil; D, photoluminescence detector; S, sample prepared in 0.050 mol L-1 NaOH; DS, donor stream: 0.75 mol L-1 HCl; AS, acceptor stream: 0.050 mol L-1 NaOH; QDs, 3.01 nm MPA-CdTe quantum dots with 0.50 µmol L-1 prepared in phosphate buffer pH = 11; W, waste.
24x14mm (300 x 300 DPI)

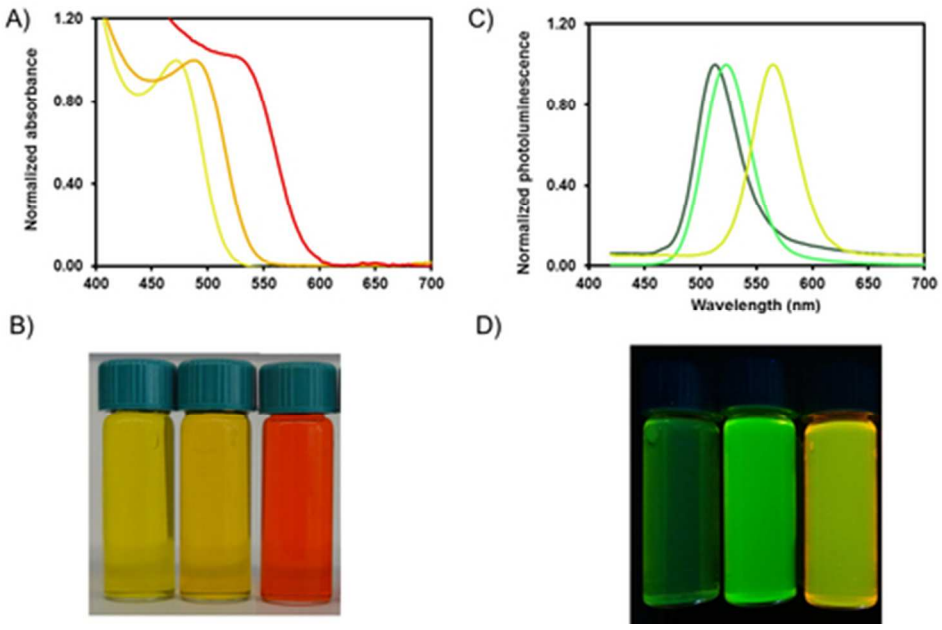

Figure 2 - Normalized UV-vis absorption (A) and photoluminescence (B) spectra of the synthesized MPA-CdTe QDs. Photograph of the QDs solutions at visible light (C) and irradiated with 365 nm light (D).
40x26mm (300 x 300 DPI)

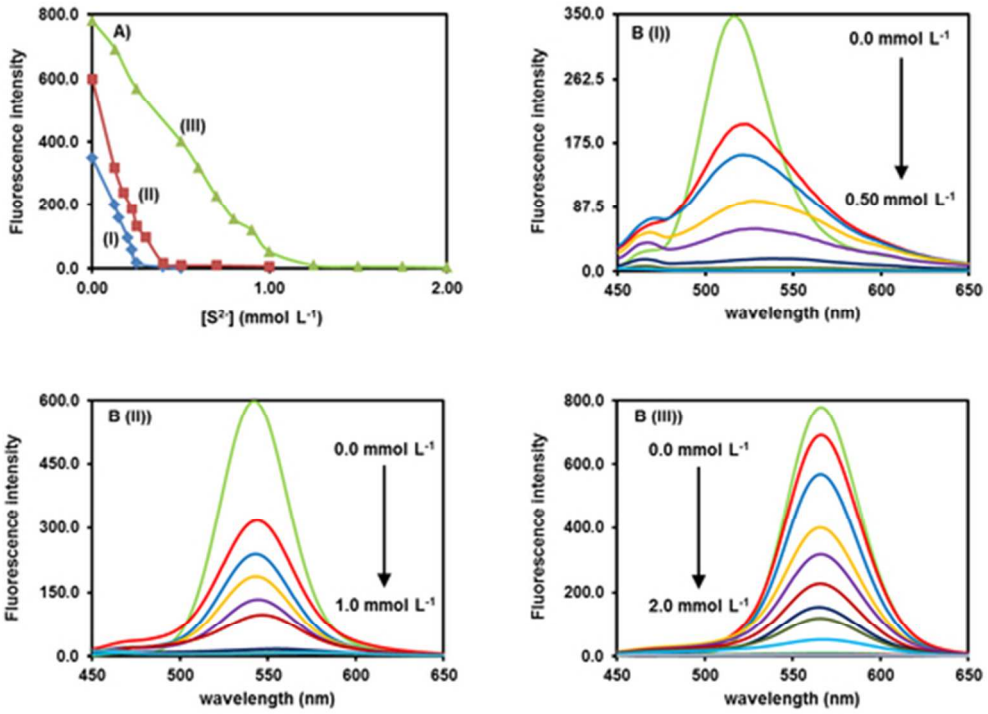

Figure 3 – A) Influence of the sulphide anion concentration on the luminescence properties of 0.5 μmol L-1 MPA-CdTe QDs with different sizes: (τ) 1.36 nm; (ν) 1.98 nm and (▲) 3.01 nm. B) Photoluminescence emission spectra of 0.5 μmol L-1 MPA-CdTe with a size of (I) 1.36 nm; (II) 1.98 nm; (III) 3.01 nm, in the presence of different S2- concentrations.
44x32mm (300 x 300 DPI)

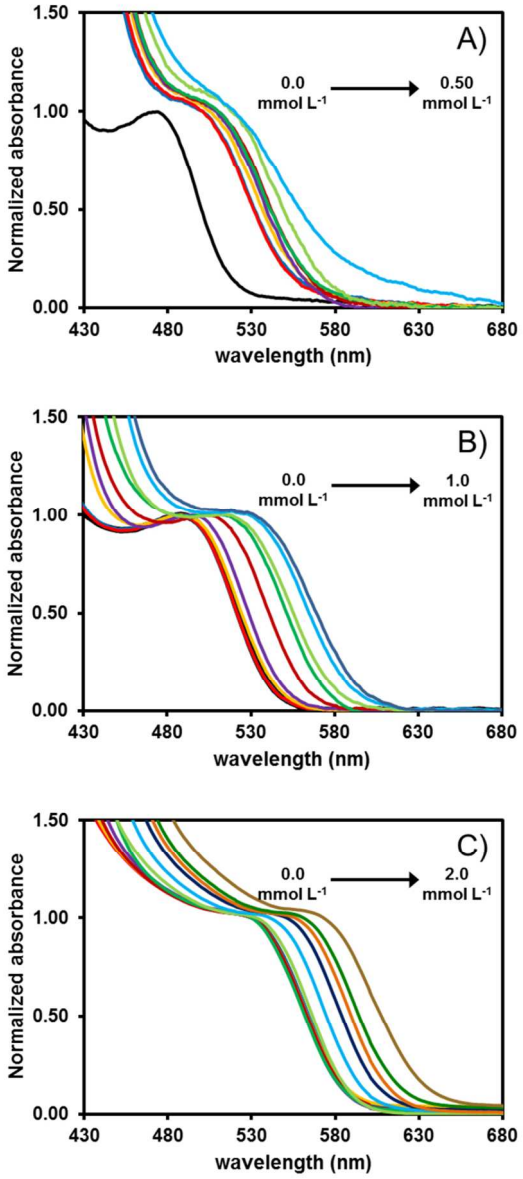

Figure 4 – Normalized UV-vis absorption spectra of 0.5 μmol L-1 MPA-CdTe with a size of (A) 1.36 nm; (B) 1.98 nm; (C) 3.01 nm, in the presence of different S2- concentrations.
63x137mm (300 x 300 DPI)

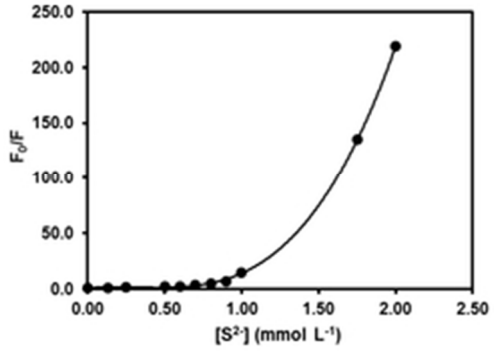

Figure 5 – Stern-Volmer plot fit curve of the interaction between the 3.01 nm MPA-CdTe QDs and sulphide anion at different concentration levels.
20x15mm (300 x 300 DPI)

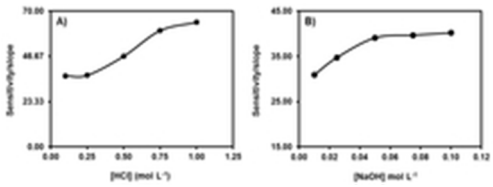

Figure 6 – Influence of (A) HCl and (B) NaOH concentrations on the sensitivity of the methodology.
20x7mm (300 x 300 DPI)

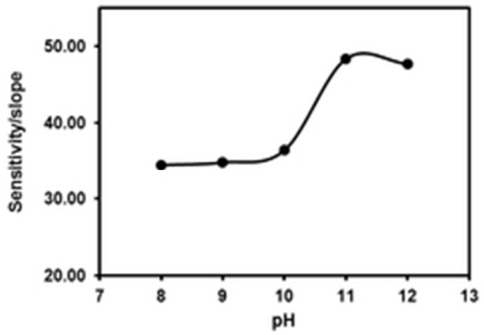

Figure 7 - Influence of the pH of QDs solutions on the sensitivity of the analytical methodology.
20x15mm (300 x 300 DPI)

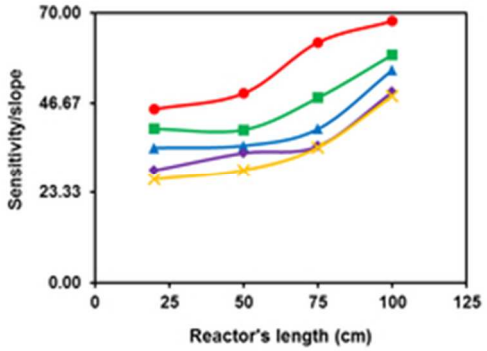

Figure 8 – Influence of the reactor's length and QDs volumes (number of pulses) on the sensitivity of the methodology. (λ) 30 µL (3 pulses); (ν) 50 µL (5 pulses); (▲) 70 µL (7 pulses); (τ) 90 µL (9 pulses) and (×) 110 µL (11 pulses).
20x15mm (300 x 300 DPI)

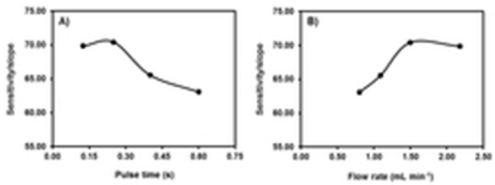

Figure 9 - Influence of the (A) pulse time and (B) the corresponding flow rate on the sensitivity of the methodology.
20x7mm (300 x 300 DPI)

Table 1 - Photoluminescence lifetime values for 0.5 μmol L^{-1} of 3.01 nm QDs with Na_2S.

$[Na_2S]_{added}$ (mmol L^{-1})	τ (ns)
0.0	43.52 ± 0.38
0.25	38.11 ± 0.58
0.50	30.36 ± 0.61
0.75	28.20 ± 0.23

Table 2 – Comparison of the results obtained in the determination of S^{2-} ion in hydrothermal waters by the proposed GD-MPFS and the reference method. Recovery tests for sulphide in spiked samples.

Sample	GD – MPFS			Reference method	
	Concentration (mmol L^{-1})		Recovery (%)	Concentration found (mmol L^{-1})[a]	R.D.[b] (%)
	added	found[a]			
Hydrothermal water 1	0.0	0.439 ± 0.009	---	0.45 ± 0.08	-2.28
	0.50	0.92 ± 0.01	96.4	---	---
	2.0	2.43 ± 0.03	99.6	---	---
Hydrothermal water 2	0.0	0.37 ± 0.03	---	0.38 ± 0.09	1.64
	0.50	0.88 ± 0.05	103.0	---	---
	2.0	2.35 ± 0.09	99.3	---	---
Hydrothermal water 3	0.0	0.58 ± 0.08	---	0.59 ± 0.09	-2.07
	0.50	1.10 ± 0.07	103.8	---	---
	2.0	2.57 ± 0.09	99.50	---	---
Hydrothermal water 4	0.0	0.40 ± 0.02	---	0.41 ± 0.07	-2.23
	0.50	0.89 ± 0.04	98.0	---	---
	2.0	2.38 ± 0.07	98.8	---	---
Hydrothermal water 5	0.0	0.379 ± 0.008	---	0.39 ± 0.05	-2.57
	0.50	0.90 ± 0.02	104.8	---	---
	2.0	2.40 ± 0.06	101.0	---	---
Hydrothermal water 6	0.0	0.34 ± 0.01	---	0.33 ± 0.07	3.24
	0.50	0.88 ± 0.05	108.0	---	---
	2.0	2.36 ± 0.05	101.0	---	---
Hydrothermal water 7	0.0	0.38 ± 0.02	---	0.38 ± 0.06	1.06
	0.50	0.87 ± 0.03	97.6	---	---
	2.0	2.43 ± 0.06	102.4	---	---

a Mean ± t0.05 (Student's t-test) × (S.D./√n).

b Relative deviation of the developed method regarding the reference procedure.

Table 3 – Results obtained for the determination of S^{2-} ion in white wines and in spiked samples through the developed GD-MPFS.

Sample	Concentration added (mmol L^{-1})	Concentration found (mmol L^{-1})[a]	Recovery (%)
Wine 1	0.0	< LOD	---
	0.50	0.52 ± 0.06	103.5
	2.0	2.1 ± 0.2	106.3
Wine 2	0.0	< LOD	---
	0.50	0.53 ± 0.01	105.1
	2.0	1.9 ± 0.1	94.9
Wine 3	0.0	< LOD	---
	0.50	0.53 ± 0.01	105.9
	2.0	1.92 ± 0.08	96.0
Wine 4	0.0	< LOD	---
	0.50	0.49 ± 0.02	97.5
	2.0	2.1 ± 0.1	103.4
Wine 5	0.0	< LOD	---
	0.50	0.49 ± 0.02	97.6
	2.0	1.97 ± 0.03	98.3

a Mean ± t0.05 (Student's t-test) × (S.D./√n).